Flavonoids Kaempferol and Quercetin are Nuclear Receptor 4A1 (NR4A1, Nur77) Ligands and inhibit Rhabdomyosarcoma Cell and Tumor Growth

Rupesh Shrestha
Texas A&M University College Station: Texas A&M University
Kumaravel Mohankumar
Texas A&M University College Station: Texas A&M University
Greg Martin
Texas A&M University College Station: Texas A&M University
Amanuel Hailemariam
Texas A&M University College Station: Texas A&M University
Syng-ook Lee
Keimyung University
Un-ho Jin
Texas A&M University College Station: Texas A&M University
Robert Burghardt
Texas A&M University College Station: Texas A&M University
Stephen Safe (ssafe@cvm.tamu.edu)
Texas A&M University

Research Article

Keywords: kaempferol, quercetin, Rhabdomyosarcoma, NR4A1, anticancer

Posted Date: June 25th, 2021

DOI: https://doi.org/10.21203/rs.3.rs-638373/v1

Version of Record: A version of this preprint was published at Journal of Experimental & Clinical Cancer Research on December 1st, 2021. See the published version at https://doi.org/10.1186/s13046-021-02199-9.

Abstract

Background

Flavonoid's exhibit both chemopreventive and chemotherapeutic activity for multiple tumor types, however, their mechanisms of action are not well defined. Based on some of their functional and gene modifying activities as anticancer agents, we hypothesized that kaempferol and quercetin were nuclear receptor 4A1 (NR4A1, Nur77) ligands and confirmed that both compounds directly bound NR4A1 with K_D values of 3.1 and 0.93 μM, respectively.

Methods

The activities of kaempferol and quercetin were determined in direct binding to NR4A1 and in NR4A1-dependent transactivation assays in Rh30 and Rh41 rhabdomyosarcoma (RMS) cells, flavonoid-dependent effects as inhibitors of cell growth, survival and invasion were determined in XTT, Annexin V and Boyden chamber assays respectively and changes in protein levels were determined by western blots. Tumor growth inhibition studies were carried out in athymic nude mice bearing Rh30 cells.

Results

Kaempferol and quercetin bind NR4A1 protein and inhibit NR4A1-dependent transactivation in RMS cells. NR4A1 also regulates RMS cell growth, survival, and invasion and pro-oncogenic PAX3-FOX01 and G9a gene expression, mTOR signaling and gene products and, these pathways and genes are inhibited by kaempferol and quercetin. Moreover, at a dose of 50 mg/kg/d kaempferol and quercetin inhibited tumor growth in athymic nude mouse xenograft model bearing Rh30 cells.

Conclusion

These results demonstrate the clinical potential for repurposing these flavonoids for clinical applications as precision medicine for treating RMS patients that express NR4A1 in order to increase the efficacy and decrease dosages of currently used cytotoxic drugs.

Background

Flavonoids are phytochemicals produced in fruits, nuts and vegetables that have been directly linked to the health promoting effects of diets enriched in flavonoid compounds. Consumption of total and individual flavonoids have been associated with increased lifetimes and protection from multiple adverse health effects including cardiovascular disease, diabetes and metabolic diseases, neurodegeneration, inflammatory diseases and cancer (1–9). For example, high dietary intakes of anthocyanins, flavonoids and flavonoid polymers by participants in the prospective Framingham Offspring cohort were correlated with lower risks of dementias including Alzheimer's disease (10, 11). Flavonoids exhibit multiple activities and the mechanisms of chemoprevention associated with high dietary intakes of flavonoids are difficult to establish. However, most dietary flavonoids exhibit antioxidant activities and they also enhance the

immune system. These effects coupled with other individual flavonoid-dependent responses contribute to their chemoprevention of diseases (12–16).

There is also evidence that diets enriched in flavonoids also protect against development of cancer (2, 4, 16–19) and this is complemented by an extensive literature on the chemotherapeutic effects of individual flavonoids. In vitro and in vivo studies demonstrate that flavonoids inhibit cancer cell growth and migration, and modulate multiple pathways and genes associated with tumorigenesis. The studies on the chemotherapeutic mechanisms associated with flavonoids as anticancer agents primarily have focused on specific functions or genes that are affected. A recent report showed that the flavonoid cardamonin inhibited dextran sodium sulfate – induced inflammation in the gut and this anti-inflammatory response was linked to the AhR activity of this compound (20). Studies in this laboratory have been investigating the pro-oncogenic roles of the nuclear orphan receptor 4A1 (NR4A1, Nur77) in rhabdomyosarcoma (RMS) and other cancer cell lines and the anticancer activities of bis-indole derived (CDIMs) which are NR4A1 ligands that act as receptor antagonists (21–27). The fusion oncogene PAX3-FOX01 and G9a have been characterized as highly pro-oncogenic factors in RMS (28, 29) and NR4A1 regulated expression of both genes and also β1-integrin and treatment of RMS cells with CDIM/NR4A1 antagonists decreased expression of these genes (21, 25). A recent study reported that the flavonoid kaempferol decreased G9a expression in gastric cancer cells (30) and this was accompanied by growth inhibition, induction of markers of apoptosis and inhibition of mTOR signaling by induced phosphorylation of AMPK. This pattern of responses observed for kaempferol in gastric cancer cells has previously been observed for CDIM/NR4A1 antagonists or NR4A1 silencing in RMS and other cancer cell lines (21–27). Therefore, we hypothesized that kaempferol is an NR4A1 ligand and this study shows for the first time that both kaempferol and quercetin bind NR4A1 and act as NR4A1 antagonists in RMS cells. Both flavonoids inhibit expression of G9a, PAX3-FOX01, and other pro-oncogenic NR4A1-regulated genes/pathways. Kaempferol and quercetin also inhibited tumor growth in an athymic nude mouse model in vivo suggesting that these nutraceuticals can be repurposed and used in a precision medicine/nutrition approach for treating RMS patients and possibly patients with other cancers that express NR4A1.

Materials And Methods

Cell lines, reagents and antibodies

The Rh30 cell line was purchased from American Type Culture Collection (Manassas, VA) and was maintained in RPMI medium. The Rh41 cell line was a generous gift from Mr. Jonas Nance, Texas Tech University Health Sciences Center- Children's Oncology Group (Lubbock, TX) and was maintained in IMDM medium. Both RPMI and IMDM media were supplemented with 10% fetal bovine serum (FBS). Cells were maintained at 37^{o}C temperature in presence of 5% CO_2. The summary of the reagents/antibodies and oligo sequences used are listed in Supplemental Tables 1 and 2 respectively. Both kaempferol and quercetin were dissolved in 100% DMSO. Rh30 and Rh41 cell lines were treated with the desired concentrations of flavonoids for 24 and 48 hours respectively. Knockdown studies by RNA interference (siNR4A1) were carried out essentially as described (21, 22).

Direct binding assay. The quenching of NR4A1 tryptophan fluorescence by direct ligand were obtained essentially as described (31); the flavonoids binding domain (LBD) of NR4A1 (0.5 μM) in buffer was incubated with different concentrations of ligands and the fluorescence was obtained using an excitation wavelength of 285 nm (excitation slit width = 5 nm) and an emission wavelength range of 300–420 nm (emission slit width = 5 nm). Ligand binding affinity (K_D) to NR4A1 was determined by measuring concentration-dependent NR4A1 tryptophan fluorescence intensity at emission wavelength of 330 nm (31).

Bis-ANS displacement assay. Bis-ANS (Molecular Probes, Inc/ThermoFisher) is essentially non-fluorescent in aqueous solution, however, bisANS fluorescence increases significantly upon binding to protein such as NR4A1. The binding affinity (K_D) and binding stoichiometry (B_{max}) of NR4A1/bisANS was determined essentially as described (32). Ligand binding affinity (K_i) to NR4A1 was determined by measuring NR4A1/bisANS fluorescence intensity at emission wavelength of 500 nm as described (32). Ligand/bisANS fluorescence intensity at each ligand concentration was used to correct the NR4A1/bisANS/ligand fluorescence intensity.

Luciferase assay

Cells (8 X 10^4) were seeded in a medium supplemented with 10% FBS and were allowed to attach to 12-well plates. After 24 hours, Lipofectamine-2000 reagent (50 umol/L) in reduced serum medium was used to co-transfect those cells with upstream activation sequence a) 400 ng $(UAS)_{x5}$-Luc and 40 ng Gal4-NR4A1 or b) 200 ng $NBRE_{x3}$-Luc and 20 ng Flag-NR4A1. The medium was removed after 6 hours and replaced with 2.5% charcoal-stripped FBS supplemented medium containing either DMSO or flavonoids. After 24 hours, the cells were lysed and the cell extract was processed for chemiluminescence quantification of luciferase activity. The Lowry protein assay was used to determine the protein concentration in the cell extract which was used to normalize the luciferase activity as described in (26, 31). Both Gal4-NR4A1 and Flag-NR4A1 that are used for this study contained full length NR4A1 coding sequence. The plasmids used for this study are constructed as described previously (26, 31).

Cell survival (XTT) assay

Cells (1 X 10^4) were seeded in 10% FBS containing medium and were allowed to attach to 96-well plates. After 24 hours, the medium was replaced with a fresh medium containing 2.5% stripped charcoal serum supplied with either DMSO or flavonoids. The XTT cell viability kit (Cell Signaling Technology, Danvers, MA) was then used and the manufacturer's protocol was followed to calculate the percentage of cell survival.

Western blot analysis

Cells treated with DMSO or flavonoids were lysed and the protein concentrations in cell extracts were quantified using the Lowry protein assay. After normalization, an equal amount of protein was loaded and allowed to run on an SDS polyacrylamide gel. The proteins from the gel were transferred to a PVDF

membrane, blocked, and incubated with the primary antibodies (overnight) followed by secondary antibodies (two hours). The HRP-substrate was then added to the membrane and the expression of the protein of interest was detected using Kodak 4000 MM Pro image station (Molecular Bioimaging, Bend, OR).

Annexin V staining

Cells were seeded and allowed to attach overnight. They were then treated with either DMSO or the desired concentration of flavonoids. Cells were then trypsinized, washed with PBS, and were then suspended in annexin binding buffer. The Annexin V and propidium iodide provided with the Alexa fluor® 488 annexin V/dead cell apoptosis kit (Invitrogen, Carlsbad, CA) were added to the cells. The manufacturer's protocol was then followed to analyze the stained cells by flow cytometry. (Data analysis was performed using FlowJo).

Migration (Scratch) assay

Cells (3 X 10^5) were seeded and were allowed to attach. After 24 hours, the medium was removed and a scratch was made on the surface using a sterile 200 µl pipette tip. The dead cells were then removed by washing the cells with PBS (2x). The medium supplemented with 2.5% charcoal stripped FBS that contained either DMSO or the desired concentration of flavonoids were then added to the cells. After 24–48 hours, the medium was removed, replaced with PBS and the pictures of migrated cells were taken using an Evos digital inverted microscope.

Boyden chamber invasion assay

Cells (2 X 10^5) were seeded and were allowed to attach to the cell culture inserts inside wells of cell culture plates. After 24 hours, the medium was removed and replaced with the fresh medium supplemented with 2.5% charcoal stripped FBS that contained either DMSO or the desired concentration of flavonoids. After 48 hours, cells were trypsinized, counted and 75,000 cells were allowed to invade through the Boyden chamber. After 24 hours, the invaded cells trapped on the lower surface of the cell culture inserts were fixed, stained and counted. At least 3 replicates were performed for each treatment group.

Spheroid invasion assay

Rh41 cells (3 X 10^3) were seeded in 200 µl 10% FBS supplemented medium in a low attachment round bottom 96 well plate. After 24 hours, when the spheroid had formed, medium (100 µL) was gently removed and the plate was allowed to chill on ice. Matrigel solution (100 µL) was then added to each well without disturbing the spheroid while the plate was still on the ice. The cells were then incubated at 37^{o}C for an hour and flavonoids (3X the desired final concentration) were added to each well. The cells were then incubated at 37^{o}C for 24 to 48 hours. After initiation of cell invasion into the Matrigel from the spheroids, medium (100 µL) was removed and replaced with 100 µl of 3X MTT solution. Cells were then

incubated at 37^{o}C for 2-hours, medium (100 µL) was then removed and replaced by 100 µL of 3.6% formaldehyde for fixation. Pictures of the invasion were then taken using an EVOS digital inverted microscope.

PCR

Cells (3 X 10^5) were seeded in a 10% FBS containing medium and were allowed to attach to 6-well plates. After 24 hours, the medium was removed and replaced with 2.5% charcoal stripped FBS supplemented medium that contained either DMSO or flavonoids. The manufacturer's protocol on Zymo Research Quick-RNA Miniprep kit (Irvine, CA) was then followed to lyse the cells and extract RNA from them. The RNA concentration in the extract was then determined, normalized and the high capacity cDNA reverse transcription kit (Thermo Fisher Scientific, Waltham, MA) was used to prepare cDNA from the isolated RNA. The amfiSure qGreen Q-PCR master mix (genDEPOT, Katy, TX) was then used to quantify the expression of mRNA of the gene of interest by quantitative real-time PCR. The human TATA binding protein mRNA was used as a control.

Chromatin immunoprecipitation assay

The manufacturer's protocol on the ChIP-IT express enzymatic kit (Active Motif, Carlsbad, CA) was followed to perform this assay. Rh30 cells were seeded and allowed to attach for 24 hours, then treated with DMSO or flavonoids for 24 hours and fixed using formaldehyde. The cross-linking reaction was stopped with glycine and the cells were lysed and nuclei were collected, sonicated, and sheared to collect chromatin fragments. These chromatin fragments were immunoprecipitated with protein specific antibodies in presence of protein G-conjugated magnetic beads. The chromatin fragments were then eluted, the protein-DNA crosslinks were reversed and digestion with protein K was performed to obtain ChIP DNA. The primers designed for specific genes were then used to perform PCR with the ChIP DNA and the amplified promoter fraction was resolved on 2% agarose gel in presence of ethidium bromide **(Denville Scientific, Metuchen, NJ)**.

Immunohistochemistry (IHC):

Tumor tissues were fixed in formaldehyde, embedded in paraffin, sectioned at 4 µM and then mounted on charged slides. These slides were deparaffinized in xylene and rehydrated through graded alcohols. Antigen retrieval was then performed and the slides were washed with Tris buffer. The IHC procedure was then performed on an automated platform (intelliPATH FLX, Biocare Medical, Pacheco, CA). All incubations were carried out at room temperature. Endogenous peroxidase activity was blocked by incubating the slides with 3% hydrogen peroxide for 10 minutes. A non-serum blocking reagent (Background Punisher, Biocare Medical) was then used to block non-specific protein binding. The Ki-67 antibody (Biocare Medical) was diluted 1:200 and incubated for 50 minutes and then a polymer detection reagent (Mach 2 HRP Polymer, Biocare Medical) was applied for 25 minutes. The sites of antigen-antibody interaction were visualized by incubating slides with a DAB chromogen (ImmPACT DAB

substrate kit, peroxidase, Vector Laboratories, Burlingame, CA) for 5 minutes. Mayer's hematoxylin was used to counterstain the sections. The slides were then dehydrated in 100% alcohol and cleared with xylene. The sections were coverslipped with a permanent mounting medium (Permount Mounting Medium, Electron Microscopy Sciences, Hatfield, PA). IHC images for Ki-67 staining were captured on a Zeiss Axio Imager.M2 motorized microscope using a 20x/0.8 NA PlanApo objective lens (Carl Zeiss Microscopy, LLC, Thornwood, NY).

Live Cell Imaging:

For imaging of live RMS cells following treatment, cells were grown on 2-well Nunc™ Lab-Tek™ II Chambered Coverglass slides with a No. 1.5 borosilicate coverglass and imaged using a motorized Zeiss Axiovert 200 MOT with a 20X 0.8 NA objective lens and DIC optics, a Roper Scientific Photometrics CoolSnap HQ Microscope Camera and incubator providing temperature and CO_2 control.

Animal studies: All the protocols for the animal studies were approved by the Institutional Animal Care and Use Committee (IACUC) at Texas A&M University. Three to four week old female athymic nude mice were purchased from Charles River Laboratories (Wilmington, MA) and were housed in the Laboratory Animal Resources and Research facility, Texas A&M University. Mice were allowed to acclimatize for a week and fed the standard chow diet. Two million Rh30 cells suspended in 100 µl of 1:1 matrigel and PBS solution were injected in each flank of the mouse subcutaneously. When the tumor size was palpable (~ 50 to 100 mm^3 in size), the mice were randomly divided into control and treatment groups. Each mouse in the control group was administered 100 µl of DMSO: corn oil (1:4) solution by intraperitoneal injection every day. Each mouse in the treatment group was injected with 100 µl of 50 mg/kg flavonoid prepared in DMSO: corn oil (1:4) solution by intraperitoneal injection every day. The mice were weighed and a Vernier Caliper was used to calculate their tumor volume (V = L*W*W/2 mm^3) every week. After the third week of drug administration, mice were sacrificed and tumors were removed and weighed. A small piece of tumor was homogenized in the lysis buffer and its extract was used for western blot analysis.

Statistical analysis

The statistical significance of differences between the treatment groups was determined by Student's t-test. Each assay was performed in triplicate and the results were presented as means with error bars representing 95% confidence intervals. Data with a *P* value of less than 0.05 were considered statistically significant.

Results

1. NR4A1 binding and transactivation induced by flavonoids

The histone methyltransferase (EHMT2) G9a is an NR4A1-regulated gene in RMS (21) and the observation that kaempferol decreased expression of G9a in gastric cancer cells (28) suggested that

kaempferol may be an NR4A1 ligand acting as an antagonist. In this study we used kaempferol and the flavonoid quercetin (Fig. 1A) and examined their activity as NR4A1 ligands in Rh30 and Rh41 RMS cells. Incubation of kaempferol and structurally related quercetin with the ligand binding domain (LBD) of NR4A1 resulted a concentration-dependent quenching of the fluorescence of Trp (31) in the LBD of NR4A1 with K_D values of 3.1 and 0.93 μM respectively (Fig. 1B and 1C). Kaempferol and quercetin also displaced the fluorescent probe bis-ANS in a competitive binding assay (33) with Ki values of 0.77 and 0.23 μM respectively (Fig. 1B and 1C). Kaempferol and quercetin also decreased transactivation in Rh30 and Rh41 cells transfected with the Gal4-NR4A1 chimera and a reporter gene (UAS-luc) containing 5 tandem yeast Gal4 response elements linked to a luciferase reporter gene (Fig. 1D). In addition, kaempferol and quercetin decreased transactivation in Rh30 and Rh41 cells transfected with an NBRE-luc reporter plasmid containing 3 tandem NBRE sites that bind NR4A1 monomer (Fig. 1E). Thus, like the CDIM/NR4A1 antagonists both kaempferol and quercetin directly bound NR4A1 and antagonized NR4A1-dependent transactivation in Rh30 and Rh41 cells.

2. Inhibition of RMS cell growth, survival, migration and invasion by flavonoids

Previous studies show that NR4A1 regulates RMS cell growth, survival and invasion, and related genes including the PAX3-FOX01 fusion oncogene and G9a (21, 25) and we therefore further investigated kaempferol and quercetin as inhibitors of these NR4A1-dependent pathways/genes. Treatment of Rh30 cells with 10–100 μM kaempferol and quercetin decreased growth (Fig. 2A) and similar effects were observed in Rh41 ARMS cells (Fig. 2B). Treatment of Rh30 cells with 25 or 50 μM kaempferol and quercetin significantly induced markers of apoptosis including cleavage of PARP and caspase 3 in Rh30 (Fig. 2C) and Rh41 (Fig. 2D) cells; these compounds also significantly induced Annexin V staining in Rh30 (Fig. 2E) and Rh41 (Fig. 2F) cells. NR4A1 knockdown or treatment with NR4A1 antagonists also inhibits RMS cell migration and invasion (21, 25) **(Supplemental Figures)** and kaempferol and quercetin inhibit migration of Rh30 (Fig. 3A) and Rh41 (Fig. 3B) cells in a scratch assay **(quantification in Supplemental Fig. 1A)**. Both flavonoid compounds also inhibited invasion of Rh30 (Fig. 3C) and Rh41 (Fig. 3D) cells in a Boyden Chamber assay and using Rh41 cells as a model 25 and 50 μM kaempferol and quercetin inhibited invasion in a 3-D spheroid invasion model (Fig. 3E). Rh30 cells did not form 3D spheroids. Thus, like CDIM/NR4A1 antagonists, kaempferol and quercetin inhibited RMS cell growth, survival, migration and invasion.

3. Inhibition of NR4A1-regulated genes by flavonoids

The histone methyltransferase G9a (EHMT2) and the PAX3-FOX01 fusion oncogene are regulated by NR4A1 in ARMS cells (21, 25) and treatment of Rh30 cells with 25 and 50 μM kaempferol and quercetin decreased expression of G9a and PAX3-FOX01 gene products (Fig. 4A). Similar results were observed in Rh41 cells (Fig. 4B). Kaempferol and quercetin also decreased expression of G9a and PAX3-FOX01 mRNA levels in Rh30 (Fig. 4C) and Rh41 (Fig. 4D) cells demonstrating that both flavonoids antagonized NR4A1-dependent gene expression in RMS cells. Both the G9a and PAX3-FOX01 promoters contain GC-rich Sp binding sites and are regulated by NR4A1/Sp where NR4A1 acts as a cofactor (21, 25). Results of

ChIP assays in (Figs. 4E and 4G) demonstrate association of NR4A1 and Sp1 with the G9a and PAX3-FOX01 promoters in untreated cells and treatment with either kaempferol or quercetin did not significantly increase or decrease NR4A1 or Sp association with the G9a and PAX3-FOX01 promoters. We also used RT-qPCR to determine fold-enrichment of the PAX3-FOX01 promoter sequence pulled down by NR4A1 and Sp1antibodies normalized to IgG antibody. Results for the G9a promoter were highly variable and this may be due to the GC-rich G9a promoter.

The histone methyltransferase gene regulates Akt phosphorylation in RMS cells (29) and NR4A1 knockdown or treatment with NR4A1 antagonists decreased G9a expression and this resulted in decreased Akt phosphorylation (pAkt). Results illustrated in Figs. 5A and 5B show that similar effects are observed for kaempferol and quercetin in Rh30 and Rh41 cells respectively. Kaempferol and quercetin also downregulate PAX3-FOX01 and PAX3-FOX01 regulated gene products (N-MYc, MyoD, Gremlin and DAPK) in Rh30 (Fig. 5C) and Rh41 (Fig. 5D) cells, and these responses were also previously observed after NR4A1 knockdown or inhibition (25) demonstrating the activity of both kaempferol and quercetin as NR4A1 antagonists. NR4A1 also regulates mTOR signaling in RMS and other cancer cell (27) lines and NR4A1 knockdown or antagonists inhibit mTOR through reactive oxygen species-dependent activation of AMPK (i.e.: pAMPK) (26, 34–36) and both kaempferol and quercetin induced pAMPK in Rh30 (Fig. 6A) and Rh41 (Fig. 6B) cells and this was accompanied by decreased phosphorylated mTOR and the downstream kinase p70S6K. NR4A1 also regulates gene products associated with attachment and migration (21–25) and treatment of Rh30 (Fig. 6C) or Rh41 (Fig. 6D) cells with kaempferol or quercetin inhibits expression of these gene products. Moreover, image analysis of Rh30 and Rh41 cells after treatment with kaempferol, quercetin (Fig. 6E) or after knockdown of NR4A1 (siRNA) identified in some changes in cell morphology and decreased cell attachment **(Supplemental Fig. 1B)**.

4. Kaempferol and quercetin inhibit RMS tumor growth in vivo

The in vivo anticancer activity of the flavonoid's quercetin and kaempferol was investigated in athymic nude mice bearing Rh30 cells as xenografts where cells were injected into the flanking region of mice. At a dose of 50 mg/kg/d, both flavonoids inhibited tumor growth (Fig. 7A) but did not affect body weights (Fig. 7B) over the 3-week treatment period. At sacrifice, tumor weights were decreased (Fig. 7C) and analysis of tumor lysates showed the expression of PAX3-FOX01 and G9a proteins were decreased (Fig. 7D) and Ki67 staining was also decreased in tumors from mice treated with quercetin and kaempferol (Fig. 7E). The complementary in vitro and in vivo studies indicate that kaempferol and quercetin are NR4A1 antagonists that are highly effective against NR4A1-dependent pro-oncogenic pathways/genes in RMS. These results suggest that NR4A1-active flavonoids can be repurposed from their broad nutriceutical applications for use as targeted agents for clinical treatment of RMS patients with tumors expressing NR4A1.

Discussion

NR4A1 is a nuclear orphan receptor with no known endogenous ligands and there is increasing evidence that this receptor and other members of this family (NR4A2 and NR4A3) play an important role in maintaining cellular homeostasis and in pathophysiology (27, 37, 38). NR4A sub-family members are typically induced by cellular stressors and in many diseases, including solid tumors where NR4A1 or other NR4A members are elevated and are potential drug targets. The role of NR4A in cancer is somewhat paradoxical (27); in many blood-derived tumors NR4A is a tumor suppressor and levels are low. Therefore, agents that induce NR4A1 and its nuclear export are potential therapeutics since the extranuclear receptor can form a proapoptotic NR4A1-bcl2 complex. In contrast, nuclear NR4A1 is pro-oncogenic in solid tumors and regulates cell growth, survival, migration/invasion and related genes (21–27, 31, 34–36). Studies on the NR4A1 antagonist activities of CDIMs demonstrate that treatment of colon, lung, breast, pancreatic, kidney, RMS, endometrial cancer cells with CDIM/NR4A1 antagonist inhibited the pro-oncogenic NR4A1-regulated functional responses **(rev in 27)**. Moreover, the effects observed after treatment with CDIMs were comparable to those observed after NR4A1 knockdown.

RMS is a cancer primarily diagnosed in adolescents and accounts for 5% of all pediatric cancers and 50% of soft tissue sarcomas in children with an overall incident rate of 4.5 x 10^6 (39–41). Embryonal RMS (ERMS) and alveolar RMS (ARMS) are the two major classes of RMS in children and adolescents and differ with respect to their histology, genetics, treatment, and prognosis (42, 43). ERMS accounts for over 60% of RMS patients and is associated with loss of heterozygosity at the 11p15 locus (42). ERMS patients have a favorable initial prognosis; however, the overall survival of patients with metastatic ERMS is only 40% (43). ARMS occur in approximately 20% of RMS patients and is associated with translocations from the fusion of *PAX3* or *PAX7* with the Forkhead gene *FOXO1* resulting in formation of pro-oncogenic gene products (44, 45). ARMS patients have a poor prognosis and patient survival is < 10% for metastatic ARMS (46). Treatments include radiotherapy, surgery, and chemotherapy with cytotoxic drugs and/or drug combinations; RMS patients that survive current cytotoxic drug therapies have a > 95% increased risk for several diseases as adults ≥ 45 years of age (47). Thus, there is a critical need for development of new therapeutic regimens for treating childhood RMS and for developing innovative therapies for treating ARMS patients since the current cytotoxic drug therapies have limited effectiveness. Our previous research has identified NR4A1 as a new drug target for treating RMS. NR4A1 is overexpressed in RMS and correlates with expression of PAX3-FOX01 in ARMS patients and treatment with synthetic CDIMs that are NR4A1 antagonists are highly effective in both cell culture and in vivo studies. The efficacy of NR4A1 antagonists is due, in part to their suppression of NR4A1-regulated mTOR signaling, PAX3-FOX01, β1-integrin and downstream gene products and the histone methyltransferase G9a (21, 25). The origins of this study were based on a recent report showing that the flavonoid kaempferol downregulated G9a in gastric cancer cells (30) and we hypothesized that kaempferol and possible other flavonoids may be NR4A1 ligands that act as receptor antagonists.

Results in Fig. 1 confirm that kaempferol and quercetin directly bind NR4A1 and competitively displace a fluorescent bound ligand (bis-ANS) and they also inhibit NR4A1-dependent transactivation. These results coupled with the effects of kaempferol and quercetin on cell growth, survival, migration and invasion

(Figs. 1–3) are also observed in RMS cells after NR4A1 knockdown or treatment with CDIM/NR4A1 antagonists (21–27).

PAX3-FOX01 and G9a are genes that play pro-oncogenic roles in RMS (28, 29) and these genes are regulated by NR4A1 which acts as a co-factor to enhance Sp1- or Sp4- mediated gene expression through NR4A1/Sp1/4 binding GC-rich promoter elements (21–25). This mechanism of NR4A1/Sp gene regulation is not uncommon and is observed for many other nuclear receptors (48). Both kaempferol and quercetin decrease expression of PAX3-FOX01 and G9a mRNA and proteins and downstream gene products (Fig. 4). Similar results were observed for activation of pAMPK and inhibition of mTOR signaling and for inhibition of genes associated with cell attachment/migration and accompanying morphological changes (Figs. 5 and 6). We also observed that at doses of 50 mg/kg/d quercetin and kaempferol were potent inhibitors of RMS tumor growth in athymic nude mice bearing Rh30 cells injected into their flanking regions (Fig. 7). The complementary results of cell culture and in vivo studies demonstrate for the first time that kaempferol and quercetin are NR4A1 ligands that act as antagonists in RMS cells and mimic the effects of NR4A1 knockdown by RNA interference (21–25). These results suggest that NR4A1-active flavonoids can be repurposed for clinical applications in the treatment of RMS and possibly other cancers where NR4A1 is a potential drug target. This type of precision medicine/nutrition approach for using flavonoids would specifically target patients that overexpress NR4A1 and could be used clinically for increasing the efficacy and decreasing the dose of currently used cytotoxic therapies.

Conclusion

RMS patients are routinely treated with cytotoxic drug combinations which have limited effectiveness and induce serious adverse health conditions later in life. NR4A1 is a pro-oncogenic factor for RMS and synthetic NR4A1 antagonists are highly effect inhibitors of growth and invasion in both cell culture and in vivo mouse models. In this study we have identified for the first-time two flavonoids that are widely used in nutriceuticals as NR4A1 ligands that act as antagonists to block NR4A1-regulated responses in RMS. The results suggest that repurposing quercetin and kaempferol for clinical applications in treating RMS patients would not only enhance the effectiveness but also lower the dosages of currently used cytotoxic agents for treating patients with this deadly pediatric tumor.

Abbreviations

Rhabdomyosarcoma, RMS; nuclear receptor 4A1, NR4A1; AMP-activated protein kinase, AMPK; Roswell Park Memorial Institute, RPMI; Iscove's Modified Dulbecco's Media, IMDM; fetal bovine serum, FBS; Dimethyl sulfoxide, DMSO; phosphate buffered saline, PBS; Institutional Animal Care and Use Committee, IACUC; ligand binding domain, LBD; Euchromatic Histone Lysine Methyltransferase 2, EHMT2; Akt phosphorylation, pAkt; Embryonal Rhabdomyosarcoma, ERMS.

Declarations

Ethics approval and consent to participate: All animal studies were carried out according to the procedures approved by the Texas A&M University Institutional Animal Care and Use Committee.

Consent for publication: Not Applicable

Availability of data and materials: Not applicable

Competing Interest: There are no conflicts of interests to declare.

Funding: This work was funded by the NIH P30-ES029067 (S. Safe).

Authors' Contributions: R.S.: Conceptualization, data curation, formal analysis, methodology, writing-original draft, project administration, writing-review and editing. **K. M.:** Data curation, formal analysis, methodology. **U. J.:** Data curation. **G. M.:** Data curation, formal analysis. **A. H.:** Data curation, formal analysis. **S. L.:** Conceptualization and editing. **R. B.:** Data curation and editing. **S. S.:** Conceptualization, data curation, formal analysis, methodology, writing-original draft, project administration, writing-review and editing.

Acknowledgements: This work was supported by the Kleberg Foundation (S. Safe), Texas A&M AgriLife Research (S. Safe), and the Sid Kyle Chair Endowment (S. Safe). The technical assistance of Drs Gus Wright, Andrew Ambrus and Chaitali Mukherjee is gratefully acknowledged.

References

1. Panche AN, Diwan AD, Chandra SR. Flavonoids: an overview. J Nutr Sci. 2016;5:e47. doi:10.1017/jns.2016.41. PubMed PMID: 28620474; PMCID: PMC5465813. Epub 2017/06/18.
2. Niedzwiecki A, Roomi MW, Kalinovsky T, Rath M. Anticancer Efficacy of Polyphenols and Their Combinations. Nutrients. 2016;8(9). Epub 2016/09/13. doi:10.3390/nu8090552. PubMed PMID: 27618095; PMCID: PMC5037537.
3. Yu J, Bi X, Yu B, Chen D. Isoflavones: Anti-Inflammatory Benefit and Possible Caveats. Nutrients. 2016;8(6). Epub 2016/06/15. doi: 10.3390/nu8060361. PubMed PMID: 27294954; PMCID: PMC4924202.
4. Kikuchi H, Yuan B, Hu X, Okazaki M. Chemopreventive and anticancer activity of flavonoids and its possibility for clinical use by combining with conventional chemotherapeutic agents. Am J Cancer Res. 2019;9(8):1517–35. Epub 2019/09/10. PubMed PMID: 31497340; PMCID: PMC6726994.
5. Krizova L, Dadakova K, Kasparovska J, Kasparovsky T, Isoflavones. Molecules. 2019;24(6). Epub 2019/03/22. doi: 10.3390/molecules24061076. PubMed PMID: 30893792; PMCID: PMC6470817.
6. Kopustinskiene DM, Jakstas V, Savickas A, Bernatoniene J. Flavonoids as Anticancer Agents. Nutrients. 2020;12(2). Epub 2020/02/16. doi: 10.3390/nu12020457. PubMed PMID: 32059369; PMCID: PMC7071196.

7. Liu Y, Weng W, Gao R, Liu Y. New Insights for Cellular and Molecular Mechanisms of Aging and Aging-Related Diseases: Herbal Medicine as Potential Therapeutic Approach. Oxid Med Cell Longev. 2019. doi:10.1155/2019/4598167. PubMed PMID: 31915506; PMCID: PMC6930799. ;2019:4598167. Epub 2020/01/10.
8. Liu XM, Liu YJ, Huang Y, Yu HJ, Yuan S, Tang BW, Wang PG, He QQ. Dietary total flavonoids intake and risk of mortality from all causes and cardiovascular disease in the general population: A systematic review and meta-analysis of cohort studies. Molecular nutrition & food research. 2017;61(6). Epub 2017/01/06. doi: 10.1002/mnfr.201601003. PubMed PMID: 28054441.
9. Caro-Ordieres T, Marin-Royo G, Opazo-Rios L, Jimenez-Castilla L, Moreno JA, Gomez-Guerrero C, Egido J. The Coming Age of Flavonoids in the Treatment of Diabetic Complications. J Clin Med. 2020;9(2). Epub 2020/02/06. doi:10.3390/jcm9020346. PubMed PMID: 32012726; PMCID: PMC7074336.
10. Shishtar E, Rogers GT, Blumberg JB, Au R, Jacques PF. Long-term dietary flavonoid intake and risk of Alzheimer disease and related dementias in the Framingham Offspring Cohort. Am J Clin Nutr. 2020;112(2):343–53. doi:10.1093/ajcn/nqaa079. PubMed PMID: 32320019; PMCID: PMC7398772. Epub 2020/04/23.
11. Shishtar E, Rogers GT, Blumberg JB, Au R, DeCarli C, Jacques PF. Flavonoid Intake and MRI Markers of Brain Health in the Framingham Offspring Cohort. J Nutr. 2020;150(6):1545–53. doi:10.1093/jn/nxaa068. PubMed PMID: 32211795; PMCID: PMC7269753. Epub 2020/03/27.
12. Maleki SJ, Crespo JF, Cabanillas B. Anti-inflammatory effects of flavonoids. Food Chem. 2019;299:125124. Epub 2019/07/10. doi: 10.1016/j.foodchem.2019.125124. PubMed PMID: 31288163.
13. Martinez G, Mijares MR, De Sanctis JB. Effects of Flavonoids and Its Derivatives on Immune Cell Responses. Recent Pat Inflamm Allergy Drug Discov. 2019;13(2):84–104. doi:10.2174/1872213X13666190426164124. PubMed PMID: 31814545. Epub 2019/12/10.
14. Sharma S, Naura AS. Potential of phytochemicals as immune-regulatory compounds in atopic diseases: A review. Biochem Pharmacol. 2020;173:113790. doi:10.1016/j.bcp.2019.113790. PubMed PMID: 31911090. Epub 2020/01/09.
15. Focaccetti C, Izzi V, Benvenuto M, Fazi S, Ciuffa S, Giganti MG, Potenza V, Manzari V, Modesti A, Bei R. Polyphenols as Immunomodulatory Compounds in the Tumor Microenvironment: Friends or Foes? Int J Mol Sci. 2019;20(7). Epub 2019/04/10. doi:10.3390/ijms20071714. PubMed PMID: 30959898; PMCID: PMC6479528.
16. Safe SJ, Chapkin A, Howard R, Mohankumaravel M, Shrestha K. R. Flavonoids: structure-function and mechanisms of action and opportunities for drug development. Toxicol Res. 2021.
17. Abbaszadeh H, Keikhaei B, Mottaghi S. A review of molecular mechanisms involved in anticancer and antiangiogenic effects of natural polyphenolic compounds. Phytother Res. 2019;33(8):2002–14. doi:10.1002/ptr.6403. PubMed PMID: 31373113. Epub 2019/08/03.

18. Abotaleb M, Samuel SM, Varghese E, Varghese S, Kubatka P, Liskova A, Busselberg D. Flavonoids in Cancer and Apoptosis. Cancers (Basel). 2018;11(1). Epub 2019/01/02. doi:10.3390/cancers11010028. PubMed PMID: 30597838; PMCID: PMC6357032.
19. Bisol A, de Campos PS, Lamers ML. Flavonoids as anticancer therapies: A systematic review of clinical trials. Phytother Res. 2020;34(3):568–82. doi:10.1002/ptr.6551. PubMed PMID: 31752046. Epub 2019/11/22.
20. Wang K, Lv Q, Miao YM, Qiao SM, Dai Y, Wei ZF. Cardamonin, a natural flavone, alleviates inflammatory bowel disease by the inhibition of NLRP3 inflammasome activation via an AhR/Nrf2/NQO1 pathway. Biochem Pharmacol. 2018;155:494–509. doi:10.1016/j.bcp.2018.07.039. PubMed PMID: 30071202. Epub 2018/08/03.
21. Shrestha R, Mohankumar K, Jin UH, Martin GG, Safe S. The Histone Methyltransferase Gene G9a Is Regulated by Nuclear Receptor 4a1 (Nr4a1) in Alveolar Rhabdomyosarcoma Cells. Molecular cancer therapeutics. 2020. Epub 2020/12/06. doi: 10.1158/1535-7163.MCT-20-0474. PubMed PMID: 33277444.
22. Shrestha R, Mohankumar K, Safe S. Bis-indole derived nuclear receptor 4A1 (NR4A1) antagonists inhibit TGFbeta-induced invasion of embryonal rhabdomyosarcoma cells. Am J Cancer Res. 2020;10(8):2495–509. Epub 2020/09/10. PubMed PMID: 32905449; PMCID: PMC7471359.
23. Hedrick E, Mohankumar K, Lacey A, Safe S. Inhibition of NR4A1 Promotes ROS Accumulation and IL24-Dependent Growth Arrest in Rhabdomyosarcoma. Molecular cancer research: MCR. 2019;17(11):2221–32. doi:10.1158/1541-7786.MCR-19-0408. PubMed PMID: 31462501; PMCID: PMC6825581. Epub 2019/08/30.
24. Lacey A, Hedrick E, Cheng Y, Mohankumar K, Warren M, Safe S. Interleukin-24 (IL24) Is Suppressed by PAX3-FOXO1 and Is a Novel Therapy for Rhabdomyosarcoma. Mol Cancer Ther. 2018;17(12):2756–66. doi:10.1158/1535-7163.MCT-18-0118. PubMed PMID: 30190424; PMCID: PMC6279487. Epub 2018/09/08.
25. Lacey A, Rodrigues-Hoffman A, Safe S. PAX3-FOXO1A Expression in Rhabdomyosarcoma Is Driven by the Targetable Nuclear Receptor NR4A1. Cancer research. 2017;77(3):732–41. doi:10.1158/0008-5472.CAN-16-1546. PubMed PMID: 27864345; PMCID: PMC5290192. Epub 2016/11/20.
26. Lacey A, Hedrick E, Li X, Patel K, Doddapaneni R, Singh M, Safe S. Nuclear receptor 4A1 (NR4A1) as a drug target for treating rhabdomyosarcoma (RMS). Oncotarget. 2016;7(21):31257–69. doi:10.18632/oncotarget.9112. PubMed PMID: 27144436; PMCID: PMC5058754. Epub 2016/05/05.
27. Safe S, Karki K. The Paradoxical Roles of Orphan Nuclear Receptor 4A (NR4A) in Cancer. Molecular cancer research: MCR. 2020. Epub 2020/10/28. doi: 10.1158/1541-7786.MCR-20-0707. PubMed PMID: 33106376.
28. Marshall AD, Grosveld GC. Alveolar rhabdomyosarcoma - The molecular drivers of PAX3/7-FOXO1-induced tumorigenesis. Skelet Muscle. 2012;2(1):25. doi:10.1186/2044-5040-2-25. PubMed PMID: 23206814; PMCID: PMC3564712. Epub 2012/12/05.

29. Bhat AV, Palanichamy Kala M, Rao VK, Pignata L, Lim HJ, Suriyamurthy S, Chang KT, Lee VK, Guccione E, Taneja R. Epigenetic Regulation of the PTEN-AKT-RAC1 Axis by G9a Is Critical for Tumor Growth in Alveolar Rhabdomyosarcoma. Cancer research. 2019;79(9):2232–43. doi:10.1158/0008-5472.CAN-18-2676. PubMed PMID: 30833420. Epub 2019/03/06.
30. Kim TW, Lee SY, Kim M, Cheon C, Ko SG. Kaempferol induces autophagic cell death via IRE1-JNK-CHOP pathway and inhibition of G9a in gastric cancer cells. Cell Death Dis. 2018;9(9):875. doi:10.1038/s41419-018-0930-1. PubMed PMID: 30158521; PMCID: PMC6115440. Epub 2018/08/31.
31. Lee SO, Li X, Hedrick E, Jin UH, Tjalkens RB, Backos DS, Li L, Zhang Y, Wu Q, Safe S. Diindolylmethane analogs bind NR4A1 and are NR4A1 antagonists in colon cancer cells. Molecular endocrinology. 2014;28(10):1729–39. doi:10.1210/me.2014-1102. PubMed PMID: 25099012; PMCID: 4179635.
32. Pastukhov AV, Ropson IJ. Fluorescent dyes as probes to study lipid-binding proteins. Proteins. 2003;53(3):607–15. doi:10.1002/prot.10401. PubMed PMID: 14579352. Epub 2003/10/28.
33. Friesner RA, Murphy RB, Repasky MP, Frye LL, Greenwood JR, Halgren TA, Sanschagrin PC, Mainz DT. Extra precision glide: docking and scoring incorporating a model of hydrophobic enclosure for protein-ligand complexes. J Med Chem. 2006;49(21):6177–96. doi:10.1021/jm051256o. PubMed PMID: 17034125. Epub 2006/10/13.
34. Mohankumar K, Li X, Sridharan S, Karki K, Safe S. Nuclear receptor 4A1 (NR4A1) antagonists induce ROS-dependent inhibition of mTOR signaling in endometrial cancer. Gynecol Oncol. 2019;154(1):218–27. doi:10.1016/j.ygyno.2019.04.678. PubMed PMID: 31053403; PMCID: PMC6625344. Epub 2019/05/06.
35. Hedrick E, Lee SO, Doddapaneni R, Singh M, Safe S. Nuclear receptor 4A1 (NR4A1) as a drug target for breast cancer chemotherapy. Endocrine-related Cancer. 2015. doi:10.1530/ERC-15-0063. PubMed PMID: 26229035.
36. Hedrick E, Lee SO, Kim G, Abdelrahim M, Jin UH, Safe S, Abudayyeh A. Nuclear receptor 4A1 (NR4A1) as a drug target for renal cell adenocarcinoma. PloS one. 2015;10(6):e0128308. doi:10.1371/journal.pone.0128308. PubMed PMID: 26035713; PMCID: 4452731.
37. Pearen MA, Muscat GE. Minireview. Nuclear hormone receptor 4A signaling: implications for metabolic disease. Molecular endocrinology. 2010;24(10):1891–903. doi:10.1210/me.2010-0015. PubMed PMID: 20392876; PMCID: PMC5417389. Epub 2010/04/16.
38. Kurakula K, Koenis DS, van Tiel CM, de Vries CJ. NR4A nuclear receptors are orphans but not lonesome. Biochim Biophys Acta. 2014;1843(11):2543–55. doi:10.1016/j.bbamcr.2014.06.010. PubMed PMID: 24975497. Epub 2014/07/01.
39. Paulino AC, Okcu MF. Rhabdomyosarcoma. Curr Probl Cancer. 2008;32(1):7–34. Epub 2008/01/22. doi: 10.1016/j.currproblcancer.2007.11.001. PubMed PMID: 18206520.
40. Breitfeld PP, Meyer WH. Rhabdomyosarcoma: new windows of opportunity. Oncologist. 2005;10(7):518–27. doi:10.1634/theoncologist.10-7-518. PubMed PMID: 16079319. Epub

2005/08/05.

41. Parham DM, Ellison DA. Rhabdomyosarcomas in adults and children: an update. Arch Pathol Lab Med. 2006;130(10):1454–65. Epub 2006/11/09. doi: 10.1043/1543-2165(2006)130[1454:RIAACA]2.0.CO;2. PubMed PMID: 17090187.
42. Scrable HJ, Witte DP, Lampkin BC, Cavenee WK. Chromosomal localization of the human rhabdomyosarcoma locus by mitotic recombination mapping. Nature. 1987;329(6140):645–7. doi:10.1038/329645a0. PubMed PMID: 3657988. Epub 1987/10/15.
43. Breneman JC, Lyden E, Pappo AS, Link MP, Anderson JR, Parham DM, Qualman SJ, Wharam MD, Donaldson SS, Maurer HM, Meyer WH, Baker KS, Paidas CN, Crist WM. Prognostic factors and clinical outcomes in children and adolescents with metastatic rhabdomyosarcoma–a report from the Intergroup Rhabdomyosarcoma Study IV. J Clin Oncol. 2003;21(1):78–84. Epub 2002/12/31. PubMed PMID: 12506174.
44. Barr FG, Galili N, Holick J, Biegel JA, Rovera G, Emanuel BS. Rearrangement of the PAX3 paired box gene in the paediatric solid tumour alveolar rhabdomyosarcoma. Nat Genet. 1993;3(2):113–7. doi:10.1038/ng0293-113. PubMed PMID: 8098985. Epub 1993/02/01.
45. Davis RJ, D'Cruz CM, Lovell MA, Biegel JA, Barr FG. Fusion of PAX7 to FKHR by the variant t(1;13)(p36;q14) translocation in alveolar rhabdomyosarcoma. Cancer Res. 1994;54(11):2869–72. Epub 1994/06/01. PubMed PMID: 8187070.
46. Maurer GD, Leupold JH, Schewe DM, Biller T, Kates RE, Hornung HM, Lau-Werner U, Post S, Allgayer H. Analysis of specific transcriptional regulators as early predictors of independent prognostic relevance in resected colorectal cancer. Clinical cancer research: an official journal of the American Association for Cancer Research. 2007;13(4):1123–32. doi:10.1158/1078-0432.CCR-06-1668. PubMed PMID: 17317820. Epub 2007/02/24.
47. Hudson MM, Ness KK, Gurney JG, Mulrooney DA, Chemaitilly W, Krull KR, Green DM, Armstrong GT, Nottage KA, Jones KE, Sklar CA, Srivastava DK, Robison LL. Clinical ascertainment of health outcomes among adults treated for childhood cancer. JAMA. 2013;309(22):2371–81. doi:10.1001/jama.2013.6296. PubMed PMID: 23757085; PMCID: PMC3771083. Epub 2013/06/13.
48. Safe S, Kim K. Non-classical genomic estrogen receptor (ER)/specificity protein and ER/activating protein-1 signaling pathways. J Mol Endocrinol. 2008;41(5):263–75. doi:10.1677/JME-08-0103. PubMed PMID: 18772268; PMCID: 2582054.

Figures

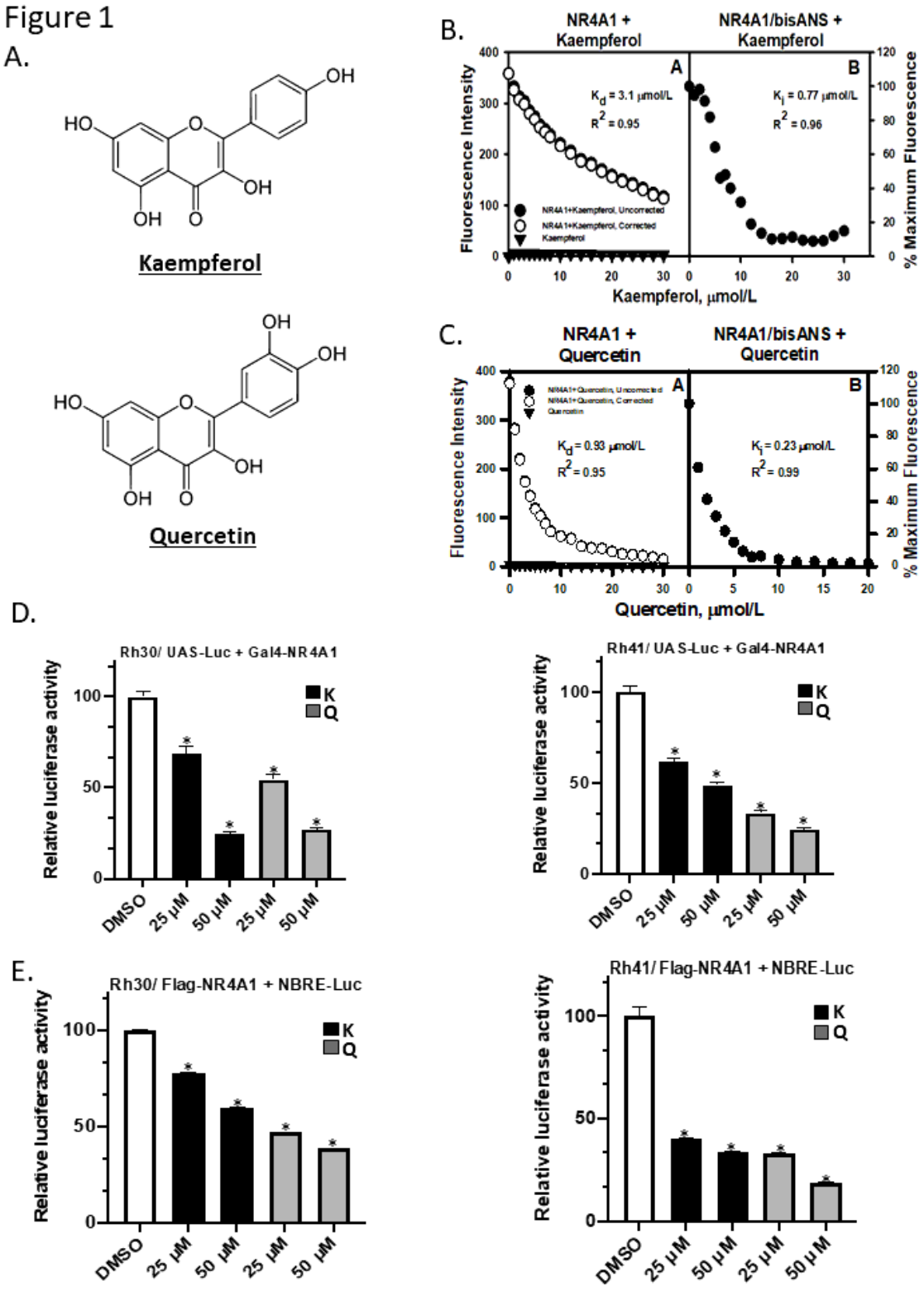

Figure 1

Kaempferol and quercetin bind NR4A1 and inhibit NR4A1-dependent transactivation. A. Structures of kaempferol and quercetin. Different concentrations of kaempferol (B) and quercetin (C) were incubated with NR4A1 (LBD) and binding was determined in fluorescent quenching direct binding or a competitive displacement (of bis-ANS) assay as outlined in the Methods. Rh30 and Rh41 cells were transfected with (D) UAS-luc/Gal4-NR4A1 or (E) an NBRE-luc/flag-NR4A1 constructs and after treatment with kaempferol

(K) or quercetin (Q) luciferase activity was determined as outlined in the Methods. Results are expressed as means ± SD for at least 3 replicated determinations and significant ($p<0.05$) inhibition is indicated (*).

Figure 2

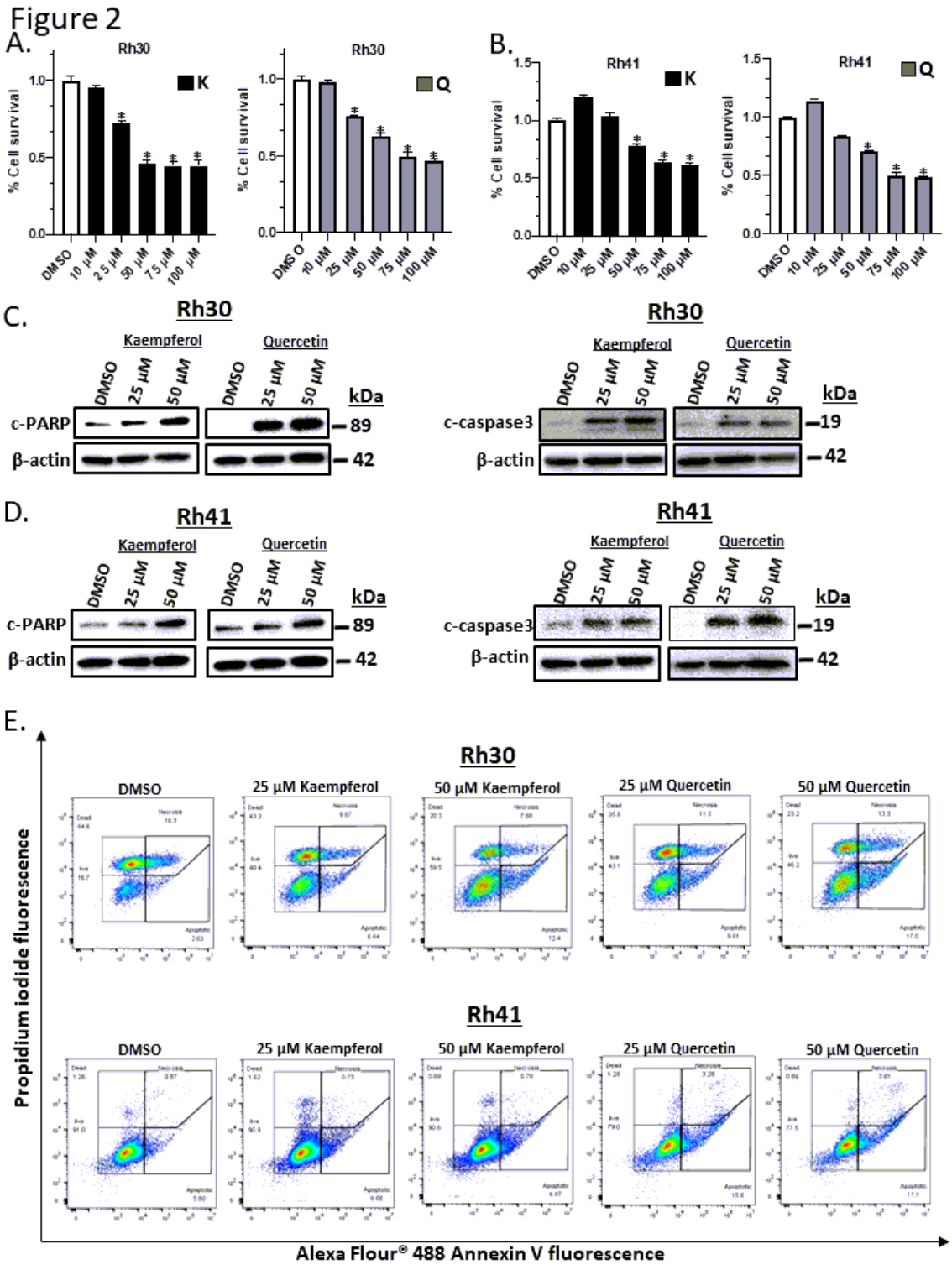

Figure 2

Kaempferol and quercetin inhibit growth and survival of RMS cells. Rh30 (A) and Rh41 (B) cells were treated with different concentrations of kaempferol (K) and quercetin (Q) and cell survival was determined as outlined in the Methods. Rh30 (C) and Rh41 (D) cells were treated with kaempferol and

quercetin and whole cell lysates were analyzed by western blot analysis as outlined in the Methods. E. Cells were treated with kaempferol or quercetin and Annexin V staining was determined as outlined in the Methods. Results (A, B) are means ± SD for at least 3 determinations and significantly ($p<0.05$) decreased growth is indicated (*).

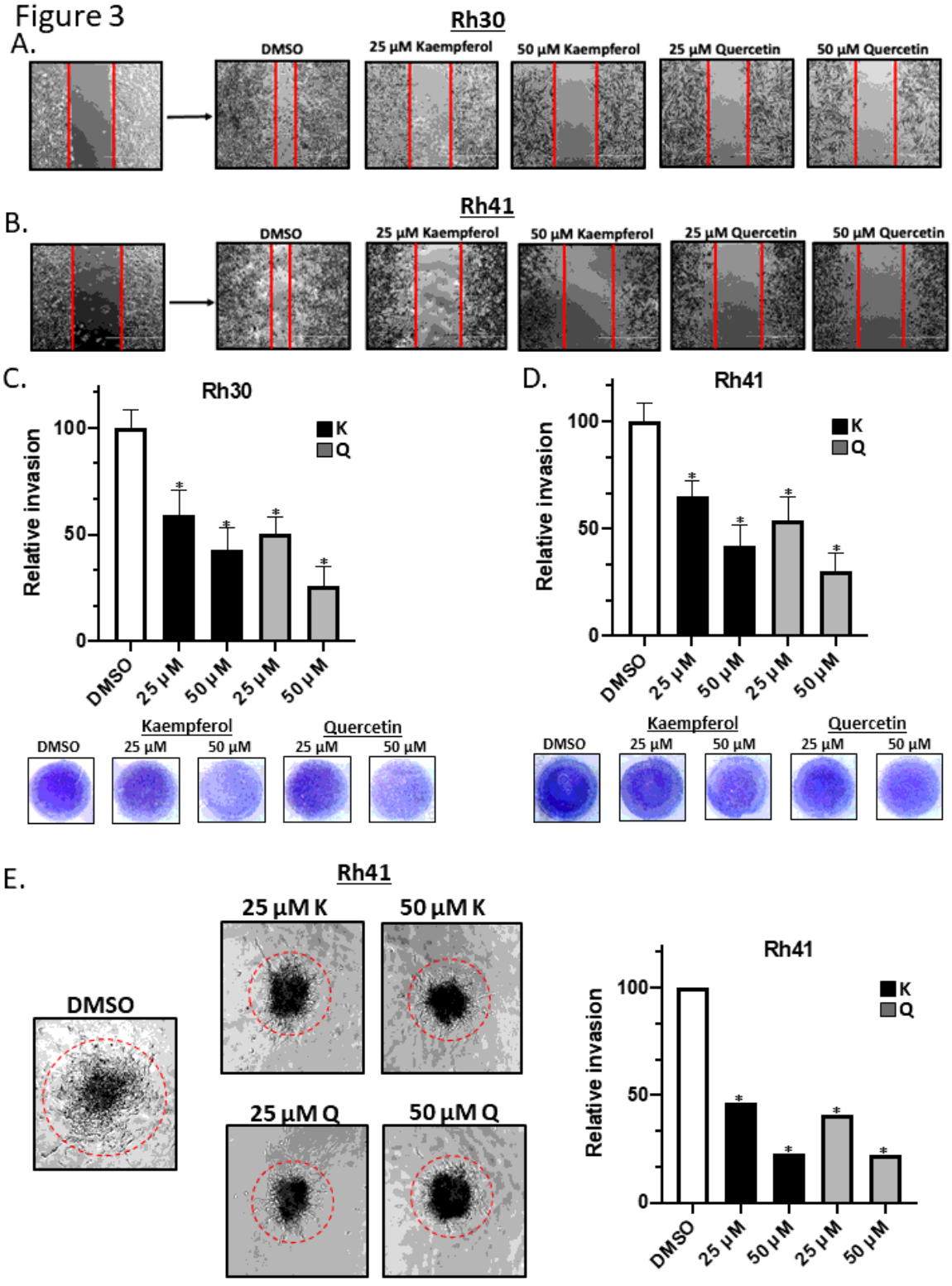

Figure 3

Kaempferol and quercetin inhibit RMS cell migration and invasion. Rh30 (A) and Rh41 (B) cells were treated with DMSO, kaempferol (K) or quercetin (Q) and effects on cell migration were determined in a scratch assay as outlined in the Methods. C. Invasion of Rh30 (C) and Rh41 (D) cells and effects of kaempferol and quercetin were determined in a Boyden chamber invasion assay and results were quantified. E. Rh41 cells were grown as spheroids and effects of kaempferol and quercetin on spheroid cell invasion were determined as outlined in the Methods. Results are expressed as means ± SD for at least 3 determinations and significant ($p<0.05$) inhibition is indicated (*).

Figure 4

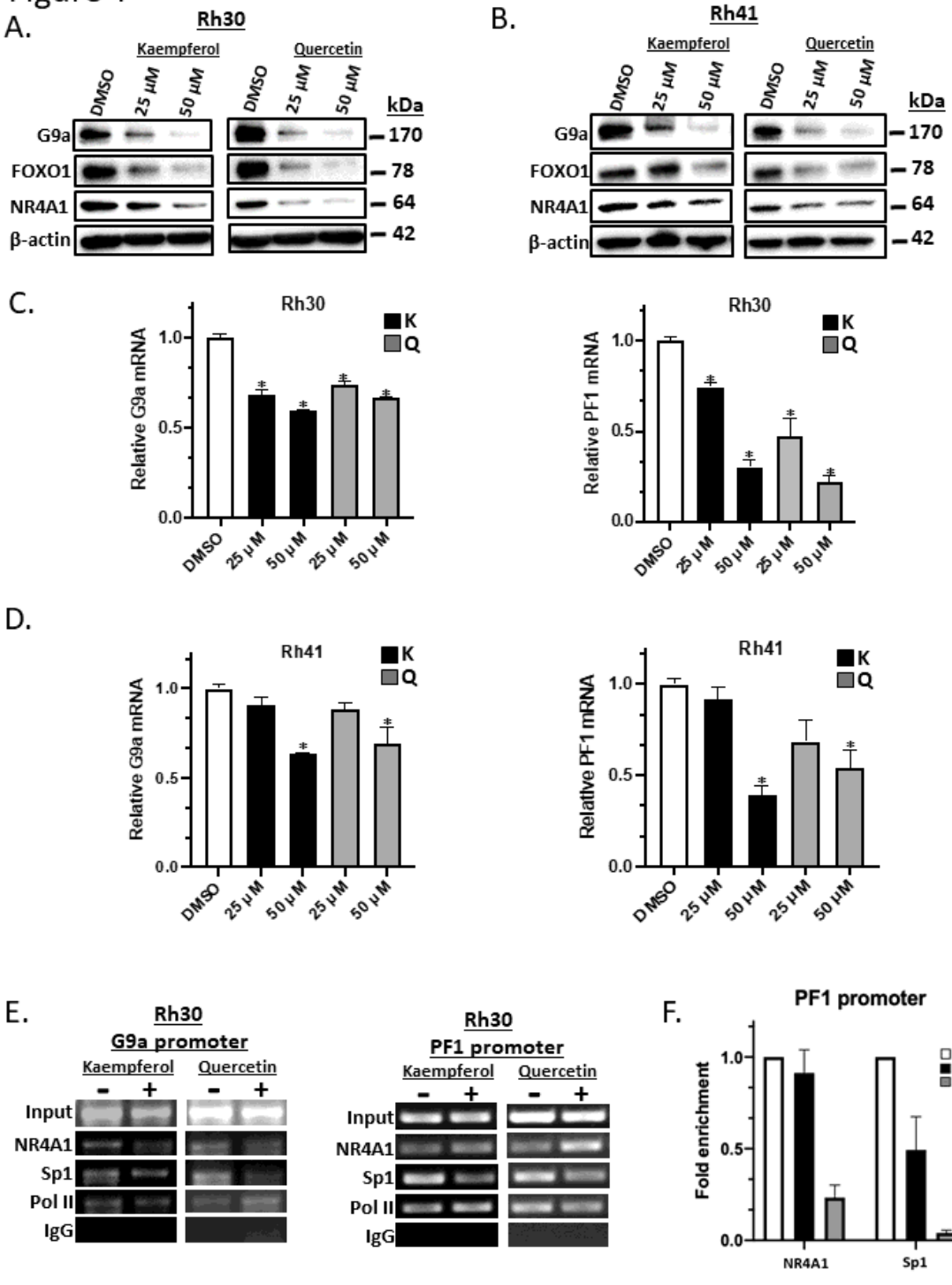

Figure 4

Kaempferol and quercetin downregulate G9a and PAX3-FOX01 in RMS cells. Rh30 (A) and Rh41 (B) cells were treated with kaempferol or quercetin and whole cell lysates were analyzed by western blots as outlined in the Methods. Rh30 (C) and Rh41 (D) cells were treated with kaempferol or quercetin and G9a and PAX3-FOX01 mRNA levels were determined by real time PCR as outlined in the Methods. E. Rh30 cells were treated with 50 μM kaempferol and quercetin for 24 hours and analyzed in a ChIP assay and the PAX3-FOX01 gene (F) was also normalized to IgG using the appropriate primers and RT-qPCR as outlined in the Methods. Results (C and D) are means ± SD for at least 3 determinations and significant ($p<0.05$) inhibition is indicated (*).

Figure 5

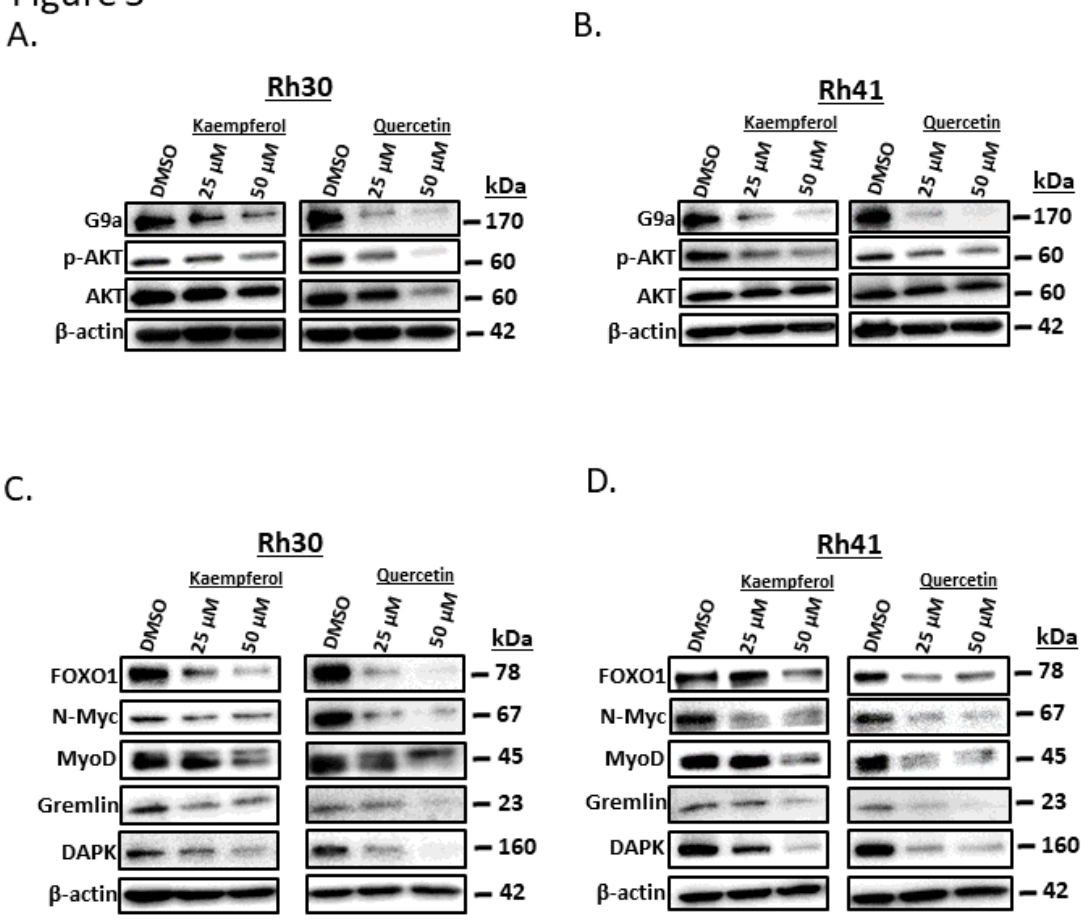

Figure 5

Kaempferol and quercetin inhibit expression of G9a- and PAX3-FOX01 – regulated gene products. Rh30 (A) and Rh41 (B) cells were treated with kaempferol or quercetin and whole cell lysates were analyzed by western blot analysis as outlined in the Methods. A similar protocol was used to determine expression of PAX3-FOX01 downstream gene products in Rh30 (C) and Rh41 (D) cells treated with kaempferol or quercetin.

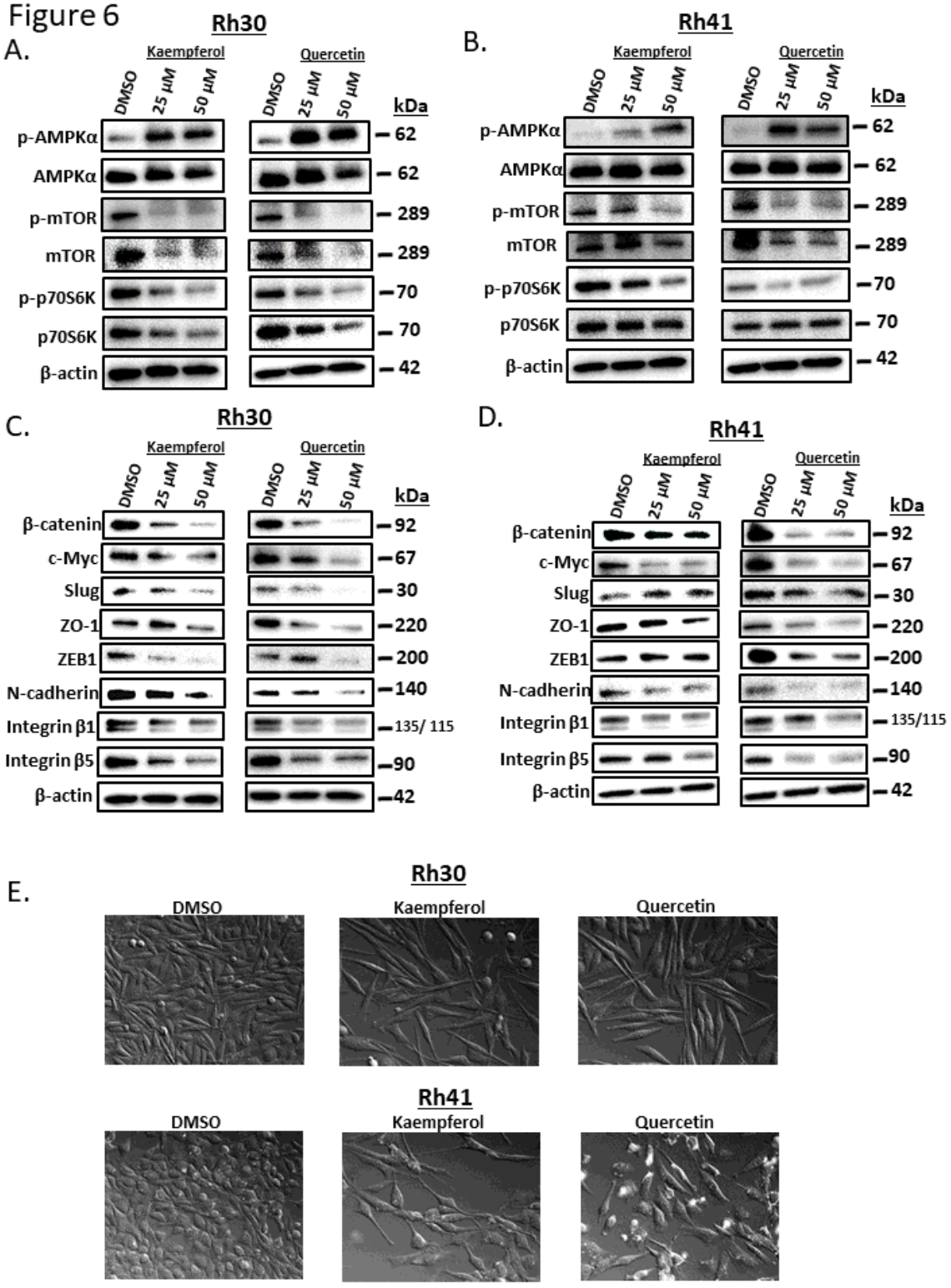

Figure 6

Kaempferol and quercetin act as mTOR inhibitors and induce cell detachment in RMS cells. Rh30 (A) and Rh41 (B) cells were treated with kaempferol or quercetin for 24 hours and whole cell lysates were analyzed by western blots. A comparable protocol was used to determine effects of kaempferol and quercetin on EMT marker gene products in Rh30 (C) and Rh41 (D) cells. E. Cells were treated with

kaempferol and quercetin and also transfected with and examined by differential interference contrast imaging as outlined in the Methods.

Figure 7

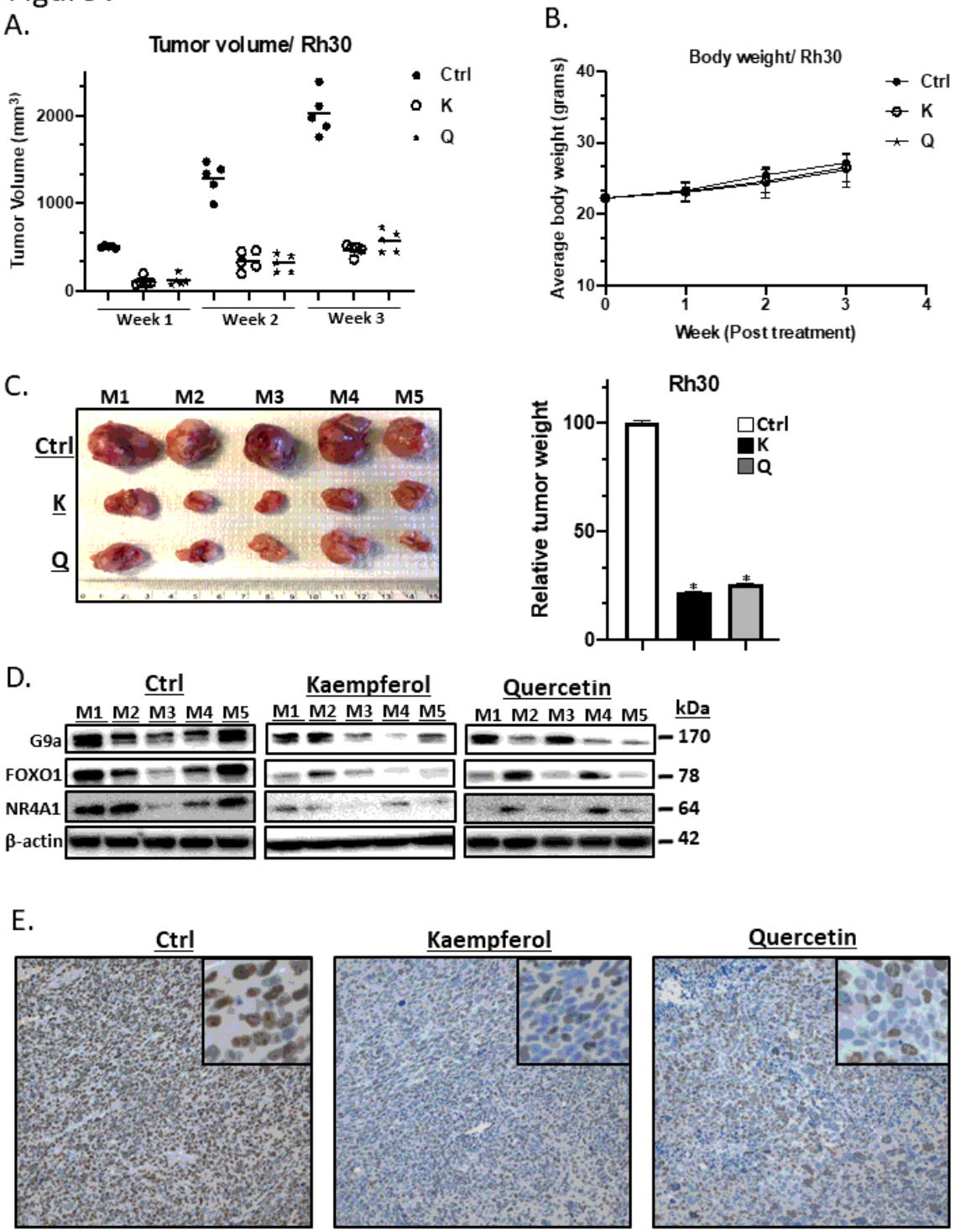

Figure 7

Kaempferol and quercetin inhibit RMS tumor growth. Rh30 cells were injected into flanks of Balb/c athymic nude mice that were treated with kaempferol or quercetin (50 mg/kg/d) by intraperitoneal injection and effects on (A) cell growth, (B) body weight changes and (C) tumor weights were determined.

D. Tumor lysates were analyzed by western blots for changes in gene expression (relative to the solvent control). E. Ki67 staining in control and treated tumor sections was determined as outlined in the Methods. Significant ($p<0.05$) flavonoid-induced effects are indicated.

Supplementary Files

This is a list of supplementary files associated with this preprint. Click to download.

- ResponsetoEditorsComments.pdf